Ising Model

Shantanu Jha and Chris West
(Dated: April 8th, 2019)

The Ising Model is an elegantly simple yet powerful model first developed to help physicists describe natural phenomena and since adopted across many disciplines. Here, we study the two-dimensional variant of the model in which two-state particles interact with each other while biased by an external magnetic field in an $N \times N$ lattice. Using a Markov Chain Monte Carlo technique to simulate averaged sampling from the Gibbs distribution characteristic of our Ising Model, we are able to study various thermodynamic properties about our lattice of particles. Perhaps the most exciting and defining of these properties is the critical temperature responsible for the discontinuities, divergences and peculiarities in our thermodynamic quantities of Magnetization, Specific Heat, Susceptibility, and Spin Correlation Length. Through our exploration of these quantities, we have found an average critical temperature $T_c = 2.29 \pm .02 J/k_B$, which almost contains the theoretical value of $T_c = 2.269$. So, we are satisfied with our T_c estimates, understanding, optimal fits and free fit parameters, such as critical exponents.

I. INTRODUCTION

A. Motivation and theory

In 1924, Ernst Ising solved the one-dimensional variant of a two-state spin model first proposed by his PhD mentor William Lenz. This model - developed to explain the phenomena of ferromagnetism - has since been adopted across dimensions and fields to describe a multitude of systems with collective behaviour [3]. The Ising model has proven to be especially successful in describing systems with simple interaction rules between homogeneous constituents each with a common external bias.

We will proceed to explore the 2D variant of the Ising Model, which consists of an $N \times N$ square lattice of nodes, each in one of two possible states ($\pm$). Given its generality, even the 2D instance of this model is useful in many fields. In physics, it is most natural to call each node a "particle" and to let each particle have a magnetization of either up or down (representing its "spin"). We then let the particles interact with their nearest neighbors with strength J[1] and be coupled to an external magnetic field of strength B. The Hamiltonian for a square lattice of side-length N can then be written as

$$\mathscr{H} = -J \sum_{\langle i,j \rangle} \sigma_i \sigma_j - B \sum_i \sigma_i \tag{I.1}$$

where $\sigma_i = \pm 1$ denotes the i-th spin state and $\langle i, j \rangle$ denotes a sum over nearest neighbors.

The particular novelty of the Ising Model is that, despite its simplicity, it exhibits a phase transition (for dimensions $d \geq 2$), something that Ernest Ising did not see in his solution for the 1D Ising Model [1]. In our exploration of the 2D Ising Model at zero applied field ($B = 0$), however, we will observe a phase transition at a critical temperature T_c. Namely, while for $T \gg T_c$ thermal fluctuations dominate and no overall magnetization is expected, we find that as $T \approx T_c$, the spins of our particles will rapidly align, leaving chunks of our lattice uniformly up or down. Then, as we have $T \ll T_c$ our lattice will develop a uniform magnetization. These three cases are depicted in Figure I.1.

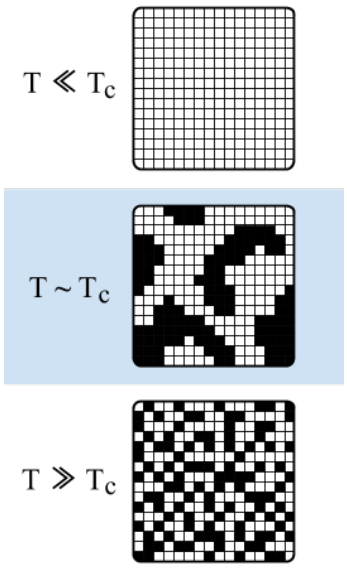

Figure I.1. The three temperature regimes for a lattice with $d = 2$. A white square represents a particle with spin $+1$ and a black square represents a particle with spin -1. Above T_c, the spins of the particles are somewhat random, leading to an expected average magnetization of 0. Near T_c, the lattice breaks into groups, all with particles of the same spin. Below T_c, the particles are either all spin $+1$ or all spin -1.

[1] Note that all J's written in the units of our graphed variables and wherever else in this report will refer to this interaction energy.

B. Simulation

Another innovation tangential to the development of the Ising Model is the creation of the Markov Chain Monte Carlo (MCMC) technique. We know from the predictions of Statistical Mechanics that the probability of finding our Ising Model in a macroscopic state of energy E is given by the Gibbs Distribution, written as:

$$\mathbb{P}(\text{state}) \propto e^{-\frac{E}{k_B T}} \tag{I.2}$$

where k_B is Boltzmann's constant and T is the temperature of the system. To better understand this notation, we can write the expected value of our energy E at some fixed temperature T, as follows:

$$\langle E \rangle_T = \frac{\sum_i E_i e^{-\beta E_i}}{\sum_i e^{-\beta E_i}} = \frac{\sum_i E_i e^{-\beta E_i}}{\mathcal{Z}} \tag{I.3}$$

where $\beta \equiv 1/(k_B T)$ and $\mathcal{Z} \equiv \sum_i e^{-\beta E_i}$ is known as the *partition function*.

Here's where we run into trouble. While the probability mass function described in Equation I.2 is computationally easy to calculate, the partition function $\mathcal{Z}$ becomes exponentially more difficult to calculate for a given temperature. We are then faced with the difficulty of how to sample accurately from the distribution of Ising Model system states at some temperature T.

The Markov Chain Monte Carlo technique is a stochastic method developed to tackle exactly this class of problems: easily described distributions, such as that of the Ising model, that are increasingly difficult to sample. As a solution, we first construct a memoryless stochastic process known as the Markov Chain. Using the Central Limit Theorem of Markov Chains, we then find that if run for a long enough time this Markov Chain will eventually closely appear to produce independent and identically distributed samples from our desired Gibbs Distribution (Equation I.2). In fact, we will be able to get samples produced from a distribution arbitrarily close to our desired Gibbs Distribution as we continue to run and *burn in* our Markov Chain. In this way, we will simulate a sampler from our desired Gibbs Distribution using a Markov Chain.

The Monte Carlo nature of our MCMC technique is used to numerically derive the average nature of our Gibbs distribution at various temperatures. We could, of course, calculate $\langle E \rangle_T$ using Equation I.3. However, as we have already discussed, the difficulty of calculating $\mathcal{Z}$ increases exponentially with our lattice size. So, we turn to the Monte Carlo technique, which averages the results of a large enough sample set from our Gibbs distribution, as simulated by our Markov Chain. Thus, we are able to sample from our desired Gibbs distribution and average many of these samples to observe the average nature of the Ising Model at various temperatures.

II. EXPERIMENTAL METHOD

While it's simple to take the limit as N goes to infinity in theory, our simulations are limited by computing power, and we can't achieve this same simplification in practice. When running the simulation, the parameters must be chosen prudently so as to maximize the effective approximating power of the model, and to minimize run time.

Perhaps the most salient parameter is N, the side-length of the square 2D lattice. Doubling N therefore quadruples the lattice size, and potentially more than quadruples run-time. We found $N = 100$ to be a good compromise; simulations could still complete in tens of minutes, and when focusing on a single observable over increasing N, dependence was minimal after about $N = 50$.

Choosing the next most important parameters - steps_anneal, steps_burnin, and EM_samples - rely on an understanding of how the output for each temperature step is collected. First, the model starts at some t_top (which we left unchanged at 4.0) and takes steps_anneal number of evenly spaced steps to the final temperature (or, in other words, the current temperature in the stepping from T_min to T_max). This technique - *simulated annealing* - is to avoid the possibility of getting randomly initialized spin lattice to get stuck in a local minimum of the Gibbs distribution. Starting at t_top guarantees the model enough energy to explore the entire probability landscape before settling to the global minimum [5]. Next, the model sits at this final temperature for steps_burnin number of steps to allow for any disillusioning effects of annealing to dissolve. Finally, EM_samples number of samples are collected. If EM_sample_spacing (call it n) is anything other than 1, the simulation will only record every n^{th} sample, while still recording a total of EM_samples (thus spending $n *$ EM_samples steps in the sampling phase for each temperature). Although using this functionality has the potential to decrease correlation between data points, we left it at 1, thinking that the binning we added to calculate c_V and χ would be sufficient section VII B. We found 50000 to be a decent value for all three of these step parameters, but would have appreciated being able to increase these further (see section VII A for an explanation).

These parameters and a couple more are summarized in Table II.1.

III. OVERALL FIT BEHAVIOR

We begin by taking a preliminary look at the entire set of data through the lens of Energy vs. Temperature and Magnetization vs. Temperature. This will exemplify some key behaviors of the Ising Model, and will motivate our analysis in later sections.

Simulation Parameter	Description	Value
N	size of the lattice	100
T_min	minimum temperature	1.2
T_max	maximum temperature	3.0
T_spacing	spacing between final temperatures	.005
steps_anneal	number of steps to take when going from the initial temperature (4.0) and the final temperature	50000
steps_burnin	number of steps to stay at the final temperature before sampling	50000
EM_samples	number of energy/magnetism samples to take, after annealing and burn-in	50000
EM_sample _spacing	option for calculating but not recording E/M data, so as to reduce correlation between subsequent data points	1
num_bins	number of data bins to use to calculate c_V and χ	50

Table II.1. A table of simulation parameters and the values they were set to for the simulation from which we collected our final data.

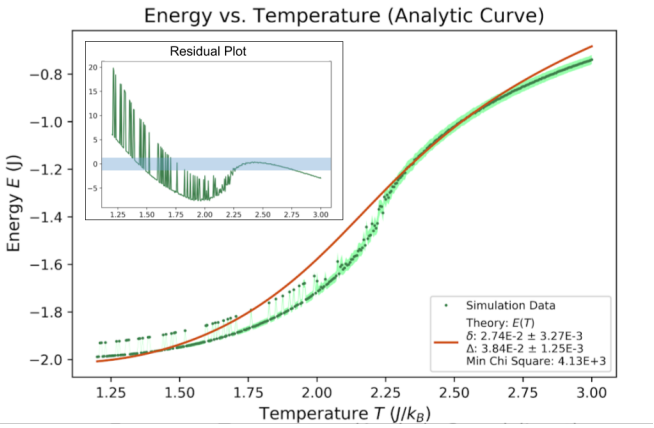

Figure III.1. Energy data (green) plotted with the theoretical curve (red), which has been fit to the data so as to take into account the finite nature of the simulation. The residuals plot includes a shaded region in the range from −1 to 1, which is the desired magnitude of the residuals. At temperatures less than the observed inflection point, there are fluctuations in the data which may be affecting the fit.

A. Energy

Of course, we expect that - generally - energy should increase with temperature. Indeed, examining the data for $E(T)$, the energy per lattice site, shown in Figure III.1 we see this increase. Further, though, we see $E(T)$ exhibiting non-linear functional behavior. Generally, this is to say that $\mathrm{d}E(T)/\mathrm{d}T$ is not constant - that the energy per lattice site changes at different rates at different temperatures. The unique behaviour of both is the first indication that the model might favor some critical temperature.

More specifically, the presence of an inflection point in the $E(T)$ data is telling. This is indicative of two things. First, that we have two distinct regions, with differing differential behavior (positive versus negative). Second, the inflection point is a point of most extreme change.

The curve graphed with the data in Figure III.1 is consistent with the analytic solution as predicted by theory. Specifically, in 1949, Lars Onsager found the following analytic solution for internal energy to the Ising Model [4].

$$E(T) = \frac{-1}{1+\Delta}\left\{2\tanh z + \frac{\sinh^2(z)-1}{\sinh(z)\cosh(z)}\left[\frac{2}{\pi}K_1(\kappa)-1\right]\right\} \tag{III.1}$$

where K_1 is a full elliptical integral of the first type and

$$z = \frac{2J}{k_B T}\frac{1}{1+\Delta},\ \kappa = \frac{2\sinh(z)}{(1+\delta)\cosh^2(z)} \tag{III.2}$$

where Δ and δ are adjustment parameters that account for the finite size of our lattice, and where in the limit as $N \to \infty$ we have that $\delta, \Delta \to 0$.

The small values of our optimal δ and Δ in Figure III.1 are reassuring in that they indicate our lattice size may be large enough to reveal 2D infinite lattice Ising model behaviour. We can also see that our theory and data, while not perfectly coincident, have similar functional forms. Both of these forms visually indicate the aforementioned special behaviour at some inflection point temperature we will later come to call T_c, which we can visually estimate to be $T_c \approx 2.25 J/k_B$.

B. Magnetization

Switching our attention to the absolute value of mean magnetization $|\langle M\rangle_T|$ graphed versus temperature in Figure III.2, we continue to see peculiar behaviour at a specific (critical) temperature we can again visually estimate to be $T_c \approx 2.25 J/k_B$. In fact, even more so than with Energy, there are two quite distinct regions our data fall into. Looking at Figure III.2 we see on the left (when $T < T_c$) the $|\langle M\rangle_T|$ values consistently at 1 while on the right (when $T > T_c$) they are consistently at 0. This almost discontinuous leap towards complete uniform magnetization in our Ising model below T_c suggests a *phase transition* as indicated by our spin arrows in Figure III.2.

We can again reference Onsanger's analytic fits of the $d = 2$ Ising Model [5], this time with the result

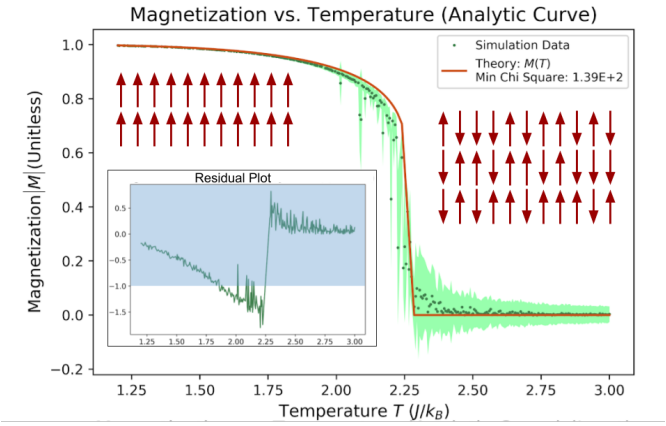

Figure III.2. Magnetization data for the full T range, with a theoretical curve set to 0 for $T > T_c$ and fitted to the data for $T < T_c$. This curve shows the phase transition perhaps most overtly, and the red arrows illustrate the model's behavior in the regime of $T > T_c$ and $T < T_c$. The low magnitude residuals give credibility to this fit.

$$\begin{cases} |\langle M\rangle_T| = \left(1 - \left[\sinh(2/T)\right]^{-4}\right)^{1/8} & T < T_c \\ |\langle M\rangle_T| = 0 & T > T_c \end{cases} \quad \text{(III.3)}$$

We can further validate our data by comparing our $|\langle M\rangle_T|$ simulated curve with theory as shown in Figure III.2. While the coincidence of our data and theory are visually convincing, we can reinforce our confidence in this data by looking at the residuals of our theory and data in Figure III.2. This residuals plot is approximately centered at 0, and does show standard normal random fluctuations.

Finally, we see that this data is furthest from our theory near T_c, since the residuals are largest in this region. Indeed, we expect irregular behavior near T_c as a product of *critical slowing* in our MCMC simulation technique near T_c [5]. As we will soon see, this irregular behaviour in combination with divergent theoretical predictions, such as that of $c_V(T)$, will make regions exceptionally close to T_c difficult to fit.

IV. CORRELATION LENGTHS

Thermodynamic fluctuations in the model can be probed by spatial correlation functions, which measure how closely two separate lattice sites are correlated. We'll consider the function

$$R(x) = \langle \sigma(0)\sigma(x)\rangle \ , \quad \text{(IV.1)}$$

which measures how likely it is that two spins separated by a distance x are aligned. $R(x) \sim 1$ indicates high correlation, while $R(x) \sim 0$ indicates low correlation. Generally, at most temperatures, $R(x)$ dies off exponentially [5] as follows:

$$R(x) \sim e^{-x/\xi} \ , \quad \text{(IV.2)}$$

where ξ is the correlation length of the system and is dependent on T. We can think of this ξ as analogous to the time constant typical of any exponential decay. A range of influence of any site in our Ising Model is then determined by this spin correlation length ξ. Namely, if ξ is small, then only spins very close to a particular site in our lattice will feel the need to align with the spin of that particular site. If ξ is larger, then this influence to align spins will extend noticeably further out.

We can plot a few graphs of $R(x)$ versus x data fitted with Equation IV.2 to gauge how this ξ changes with T.

First, we see a correlation length of $\xi(T = 1.905J/k_B < T_c) = .79 \pm .02$ in Figure IV.1. Next, we see a correlation length of $\xi(T = 2.755J/k_B > T_c) = 1.73 \pm .02$ in Figure IV.2. Both of these correlation lengths are relatively low and imply a range of influence that extends only to the immediate neighbors of a particular site in our lattice.

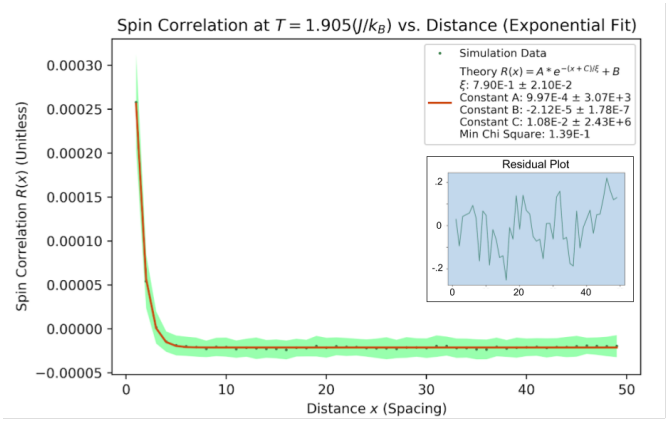

Figure IV.1. Spin Correlation data for a temperature less than T_c plotted with a χ^2 minimized $R(x)$ fit. $R(x)$ has been given translational and scaling freedom, as these are not attributes that would affect the time constant. The residuals fall within the desired range yet, since $\chi^2 = .14 \not\sim 1$, the error may be overestimated.

However, when we study the spin correlation vs. distance at $T \approx T_c$ as displayed in Figure IV.3, we find that $\xi(T = 2.24J/k_B \approx T_c) = 5.6 \pm .17$. This noticeably larger spin correlation length is indicative of a larger range of influence for each site in our lattice at $T \approx T_c$.

Theory also predicts that at $T \approx T_c$, we can conduct a power law fit for $x \ll \xi$, written as:

$$R(x) \propto |x|^{-d+2-\eta} = |x|^{-\eta} \quad \text{(IV.3)}$$

where the dimension $d = 2$ for the 2D Ising model.

Since our maximum ξ, which is reached at $T \approx T_c$, is less than 6, we will conduct a power law fit for all $x < \xi$ rather than $x << \xi$ out of a need for more data points. However, we see that our best fit curve and its

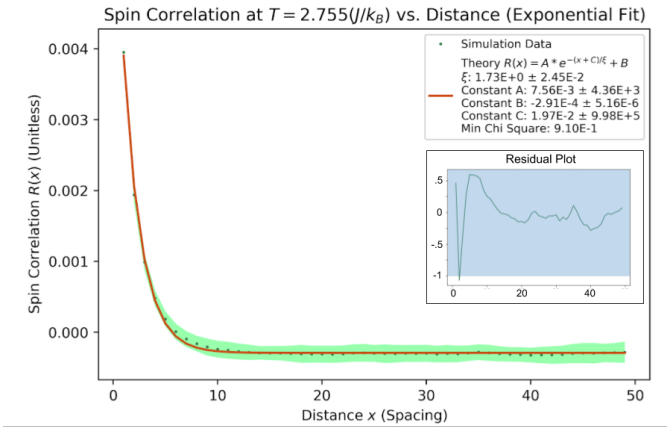

Figure IV.2. Spin Correlation data for a temperature greater than T_c plotted with a χ^2 minimized $R(x)$ fit. $R(x)$ has been given translational and scaling freedom, as these are not attributes that would affect the time constant. The residuals fall within the desired range and, since $\chi^2 = .91 \sim 1$, this appears to be a strong fit.

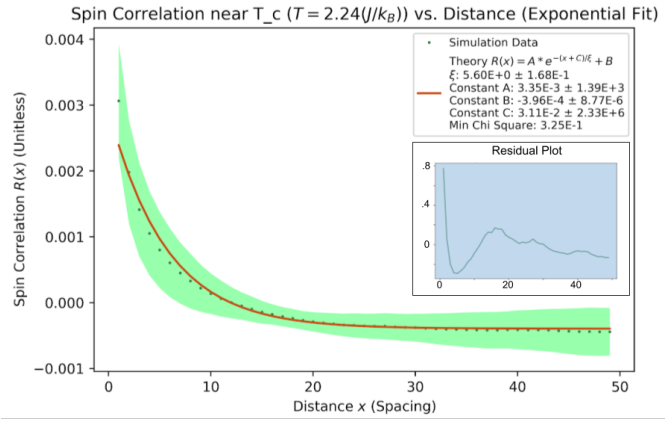

Figure IV.3. Spin Correlation data for a temperature about equal to T_c plotted with a χ^2 minimized $R(x)$ fit. Notice that correlation decays at a significantly slower rate than for T not near T_c, as shown in Figure IV.1 and Figure IV.2

.

residuals when compared to theory in Figure IV.4 look completely reasonable. The free fit parameter η, which we will later come to know as a critical exponent, has a value of $\eta = .57 \pm .03$ which is a bit off the accepted value of $\eta = .25$. The finite nature of our lattice and subsequent low maximum spin correlation length ξ at T_c or the critical slowing down near T_c of our simulation are all likely factors towards an optimal η that does not match what theory predicts. However, this is less important than the matching function form apparent between theory and data as demonstrated by Figure IV.4.

Also, it is important to know that our $R(x)$ vs. x curve in Figure IV.4 is an average of the $R(x)$ curves from a very small range of $T \approx T_c$ to both generate motivated error bars on our $R(x)$ values and to average out outliers

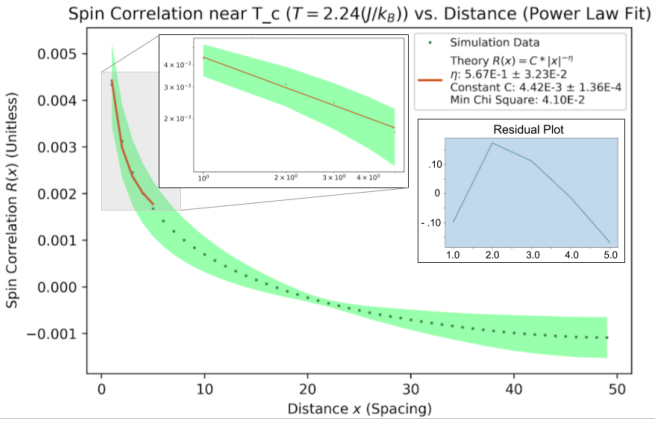

Figure IV.4. Spin Correlation data for a temperature about equal to T_c plotted with a χ^2 minimized power law fit. This fit is valid only for $x \ll N$. The low magnitude χ^2 and residuals indicate an overestimation of error.

from critical slowing down near T_c. This averaging at T around T_c may also be responsibly for overestimated error bars, leading to the very small $\chi^2_\nu = .04 << 1$ in Equation IV.4.

From the preceding discussion, we see that our correlation length seems to be negligible at $T \not\approx T_c$ and sizeable at $T \approx T_c$. Perhaps we can find some justification behind the peculiar behaviour the 2D Ising Model undergoes at $T \approx T_c$ through a detailed analysis of these correlation lengths ξ.

As depicted in Figure IV.5, we can now see how this correlation length ξ varies with T. Again, we see an irregularity near $T \approx 2.25 J/k_B \approx T_c$ (our visual estimate of T_c), which manifests as a divergence in Spin Correlation Length ξ. This divergence is predicted by theory and implies that the range of influences of our lattice sites are largest at $T \approx T_c$ where ξ is greatest. Now, we begin to see the root of the irregularities at our T_c critical temperature.

As mentioned before, our finite lattice forms chunks of uniformly magnetized spins at $T \approx T_c$, something which we can now explain with an increased desire for our particles to align with not only their neighbors but also particles far away from them but within the spin correlation length ξ. The advent of these uniformly magnetized chunks of spins can be further explained by the effect of the finite nature of our lattice on our spin correlation lengths as a function of temperature. We find that in the finite 2D lattice, the spin correlation length does not diverge at T_c, rather it peaks. This maximum value of ξ at around T_c is of the order of the radii of the chunks of uniformly magnetized spins. In the infinite lattice limit, $\xi \to \infty$ as $T \to T_c$ and instead of chunks we see a discontinuous phase transition from a completely disordered lattice to a completely uniformly magnetized lattice. Namely, we would see our infinite lattice jump from the regime of $T \gg T_c$ to that of $T << T_c$ as shown in Figure I.1, skipping the formation of chunks stage even

as we pass T_c.

To further validate our data, we can describe the spin correlation length ξ curve by the following power law fit at temperature near T_c:

$$\xi \propto |t|^{-\nu} \tag{IV.4}$$

where t is our reduced temperature defined as follows:

$$t = \frac{T - T_c}{T_c} \tag{IV.5}$$

The volatility of our ξ data below an estimated T_c compelled us to fit this power law in Equation IV.4 only for T above our estimated T_c. From this fit and the adjoining residuals graph displayed in Equation IV.4, we see that our data closely follows theoretical predictions that support this divergence of spin correlation length at T_c, which we have found to have an optimal value of $T_c \approx 2.24 \pm .02$. This is our first (of many) quantitative fit predictions of T_c, an increasingly important temperature point.

We also see an optimal $\nu = .59 \pm .11$, another critical exponent, which almost coincides with the accepted value of $\nu = 1$. This, however, is less important than the appropriate functional similarity between our theory and data as demonstrated by our plot and residuals in Figure IV.5 and a reasonable T_c optimal value.

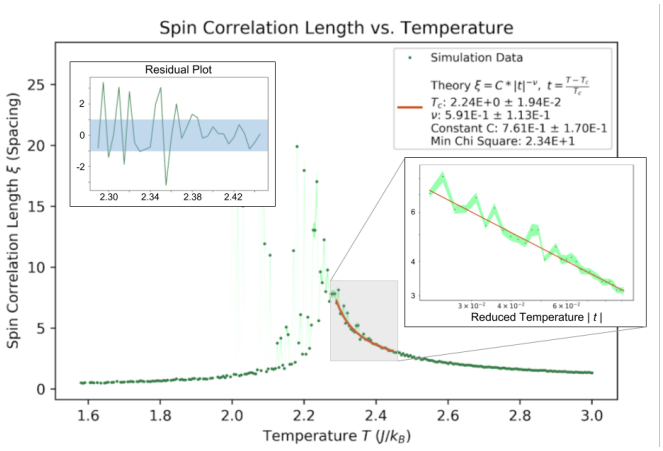

Figure IV.5. A plot of spin correlation length for the full range of temperatures. The power law fit is shown in the inset on a log-log scale. The slightly large residuals and the χ^2 of 23.4 indicate that error may be underestimate here.

V. POWER LAW FITS: AROUND T_c

We have talked at length about the peculiarities of the 2D Ising Model and the phase transition it undergoes at the critical temperature T_c. In the following section, we will continue our exploration of the data generated by the 2D Ising model, our validation of that data with theoretical fits, and our discussion of the importance of T_c and how to measure it. Many of these power law theoretical fits will also have free fit parameters called critical exponents, which when compared to accepted values will help compare our results to what is expected by theory.

A. Magnetization: near T_c

First, we will revisit the familiar data set of the absolute value of mean magnetization as a function of temperature. Like many of the curves in this section, our $|\langle M \rangle_T|$ exhibits behaviour well described by a power law fit for T right below T_c, written as:

$$|\langle M \rangle_T| = |M| \propto |t|^{\beta} \tag{V.1}$$

where t is again the reduced temperature as defined in Equation IV.5.

From this fit, we will be able to verify the functional form of our $|\langle M \rangle_T|$ curve near T_c and derive a quantitative estimate of T_c.

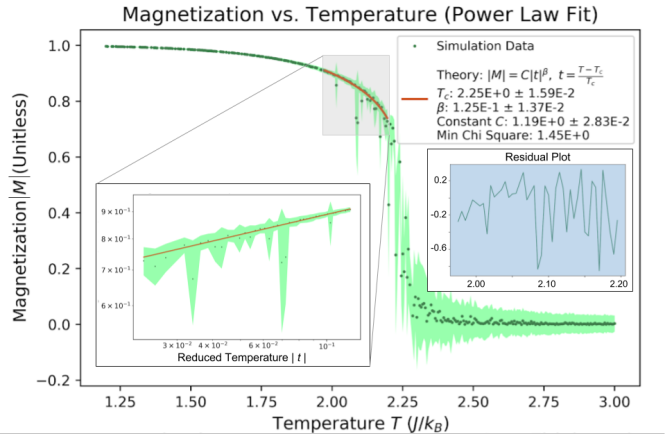

Figure V.1. Magnetization data with the power law fit for just below T_c. The inset shows the area of interest graphed on a log-log scale over the reduced temperature t. Low magnitude residuals and a χ^2 on the order of 1 both indicate that this is a good fit.

We see from Figure V.1 that $T_c = 2.25 \pm .02 J/k_B$ and $\beta = .125 \pm .01$, which is completely coincidental with the accepted β value of .125. While our residuals in Figure V.1 suggest that we have maybe overestimated our error, the validity of our critical exponent add further legitimacy to our estimate of T_c.

B. Specific Heat c_V: near T_c

The next thermodynamic quantity of interest is specific heat c_V defined as follows:

$$c_V = \frac{\partial \langle E \rangle_T}{\partial T} = \frac{\beta}{T}(\langle E^2 \rangle_T - \langle E \rangle_T^2) \tag{V.2}$$

We can now use graph c_V vs. temperature to gain insight on the validity of my data and the potential of it to yield a measure of T_c. Again, we can accomplish both by attempting to power law fit T near T_c, using the fit formula:

$$c_V \propto |t|^{-\alpha} \tag{V.3}$$

where t is again the reduced temperature as defined in Equation IV.5.

Note that because of the divergent nature of c_V near T_c and critical slowing down of T very close to T_c, our fits of c_V did not consider a small portion of $T \approx T_c$. We also tackled our fit in two portions. We first fit this power law theory for $T < T_c$ and then for $T > T_c$, with all T values reasonably close to T_c.

The first fit of $T < T_c$, as displayed in Figure V.2, yielded a $T_c = 2.23 \pm .03 J/k_B$ and $\alpha = .5 \pm .12$. The second fit of $T > T_c$ as displayed in Figure V.3, yielded a $T_c = 2.32 \pm .01$ and $\alpha = .143 \pm .04$.

When compared to the theoretically accepted value of α which is 0, our α estimates are much larger than they should be. However, we can chalk this up to the finite nature of our lattice and the fact that in this finite lattice c_V does not get to fully diverge at $T \approx T_c$, rather c_V peaks to a maximum in that region of $T \approx T_c$. Thus, while the functional form is the same, we will never be able to achieve an $\alpha = 0$ best fit for a finite lattice 2D Ising model data set.

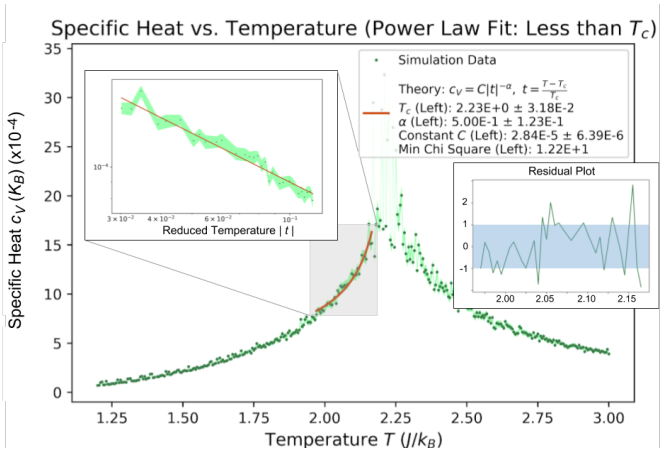

Figure V.2. Specific heat for the full range of T with a power law fit just below T_c. The inset shows the region that has been fitted on a log log scale and over reduced temperature.

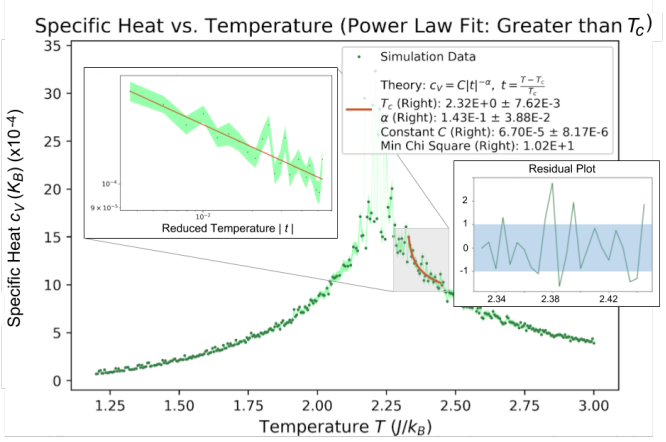

Figure V.3. Specific heat for the full range of T with a power law fit just above T_c. The inset shows the region that has been fitted on a log log scale and over reduced temperature.

C. Susceptibility χ

The last thermodynamic quantity of interest is susceptibility, defined as:

$$\chi = \frac{\partial \langle M \rangle_T}{\partial \partial B} = \beta(\langle M^2 \rangle_T - \langle M \rangle_T^2) \tag{V.4}$$

Like Specific Heat, Susceptibility diverges at T_c in the infinite lattice 2D Ising model. So, for the same reasons as before and because of added noise for $T < T_c$, we will only perform a power law fit on χ for $T > T_c$. This fit can be written as follows:

$$\chi \propto |t|^{-\gamma} , \tag{V.5}$$

where again, $|t|$ is the reduced temperature as defined in Equation IV.5.

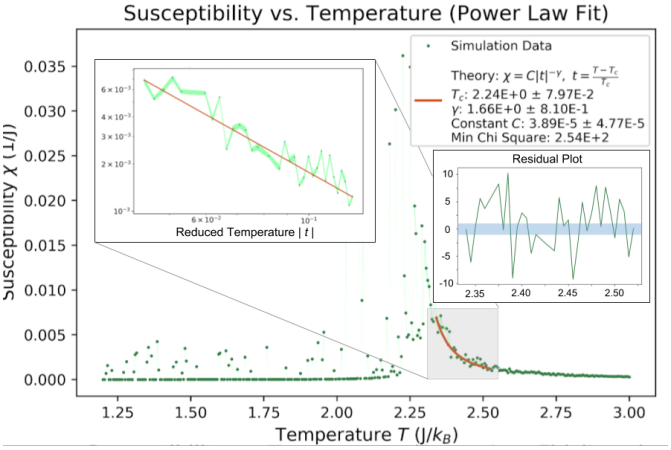

Figure V.4. Susceptibility for the full range of T with a power law fit just above T_c. The inset shows the region that has been fitted on a log log scale and over reduced temperature.

As taken from Figure V.4, we can derive a best fit $T_c = 2.24.08 J/k_B$ and $\gamma = 1.66 \pm .8$. Since $\gamma = 1.66 \pm .8$

contains the expected value of γ of 1.75, we can say with confidence that our data and T_c estimate are reasonable for susceptibility.

D. Critical Exponent Summary

We have thus completed our power law fit analysis of the various thermodynamic quantities we generated in our MCMC simulation of the 2D Ising model.

Critical Exponent	Definition	Theoretical Value	Exper. Value
α (Left)	$c_V \propto \lvert t\rvert^{-\alpha}$	0	.50 ±.12
α (Right)	$c_V \propto \lvert t\rvert^{-\alpha}$	0	.143 ±.04
β	$\lvert M\rvert \propto \lvert t\rvert^{\beta}$	1/8	.125 ±.014
γ	$\chi \propto \lvert t\rvert^{-\gamma}$	7/4	1.66 ±.81
ν	$\xi \propto \lvert t\rvert^{-\nu}$	1	.591 ±.113
η	$R(x) \propto \lvert x\rvert^{-d+2-\eta}$	1/4	.57 ±.03

Table V.1. A table of critical exponents and parameters, and their theoretical and experimental values when appropriate.

Origin	T_c Experimental Value
c_V (Left) $\propto \lvert t\rvert^{-\alpha}$	2.23 ±.03
c_V (Right) $\propto \lvert t\rvert^{-\alpha}$	2.32 ±.01
$\lvert M\rvert \propto \lvert t\rvert^{\beta}$	2.25 ±.02
$\chi \propto \lvert t\rvert^{-\gamma}$	2.24 ±.08
$\xi \propto \lvert t\rvert^{-\nu}$	2.24 ±.02
Average	2.29 ±.02

Table V.2. A table of calculated values of T_c, and from what variable they originated.

VI. CONCLUSION

We began our discussion of the Ising Model by observing the peculiarities of our $\langle E\rangle_T$ and $|\langle M\rangle_T|$ data around what we believed to be a special temperature, which we later dubbed the critical temperature T_c. After a detailed analysis of the interactions and correlations between the states in our 2-dimensional $N \times N$ lattice, we gained a better understanding of what made our critical temperature so special. We found that at this T_c, the correlation length - a sort of correlation decay constant - is theoretically peaked. Here, we also began to notice the limiting nature of the finite $N \times N$ lattice as $N \to \infty$, namely when speaking of peaks vs. divergences and of phase transitions. As our focus shifted around T_c, so did our fits. From theoretical power law curves, we were able to both test the validity of our data for various thermodynamic quantities, but also extract critical exponents and quantitative estimates for our critical temperature. Both of these metrics allowed us to verify theoretical predictions with our simulations. Like Lenz, Ising, and Onsager, we were humbled by the versatility and simple elegance of the Ising model.

VII. APPENDIX

A. Simulation Errors

As we explored larger simulations - more annealing, burn-in, and sample steps, larger N, and smaller temperature spacing - we began to encounter issues with the Ising Model code. Run after run, it appeared that all of the temperature steps were completing (and in a reasonable amount of time), yet the data was not getting written to the .csv file. At first, we suspected that between our various modifications to the code, we had messed something up. But, we encountered this error even when running the original code directly from the github. Unfortunately, given the time-frame, we were not able to determine the issue. Although we would have liked to have been able to analyze data for a temperature spacing of .001 and with annealing, burn-in, and sample steps of 100000, we are fairly happy with the data we were able to get.

B. Code Modification

We added calculations of specific heat c_V and χ (and their respective standard deviations). We used the following equations for these calculations [5]:

$$c_V = \frac{\beta}{T}\left(\langle E^2\rangle_T - \langle E\rangle_T^2\right) \tag{VII.1}$$

and

$$\chi = \beta\left(\langle M^2\rangle_T - \langle M\rangle_T^2\right) \ . \tag{VII.2}$$

To reduce the negative effect of correlation between consecutive data points, we randomly re-ordered the list of energy and magnetization values collected for each final temperature, and then split the list into 50 bins. We then stored the standard deviation for each bin, and calculated c_V and χ from there.

C. Data Analysis Discussion

The majority of our data analysis consisted of finding the best fits of our theoretical curves on our data. From these optimal fits, we were able to derive best fit parameters and compare them against accepted values.

1. *Reduced χ^2_ν Minimization*

To obtain a quantitative measure of the deviation of our data from theoretical predictions we used the χ^2_ν met-

ric. The χ^2_ν measure is a reflection of the distance of our data from a curve constructed through theoretical predictions. Specifically, we calculate the χ^2_ν as follows:

$$\chi^2_\nu = \frac{1}{\nu} \underbrace{\sum_{i=1}^{N} \frac{(y_i - f(x_i, \alpha))^2}{\sigma_i}}_{\chi^2} \tag{VII.3}$$

where y_i are our N simulated data points, $f(x_i, \alpha)$ are the y values of our theoretical curve given parameter set α, and σ_i is the uncertainty in our simulated data y_i. In addition, $\nu = N - p$ is the number of data points N minus number of parameters p we are free to change. This ν is a measure of the true degrees of freedom in our fit. By reducing our χ^2 by ν, we obtain a normalized χ^2_ν which is much easier to make sense of than our original χ^2. We also see that a larger χ^2 is acceptable if our ν, number of degrees of freedom, is larger.

Our goal is to find the set of parameters α that minimize our χ^2_ν for each fit. In our earlier analysis, we traversed a grid of parameter choices for each fit. Then, by finding the minimum of the χ^2_ν values calculated for each point on our parameter grid, we were able to ascertain the optimal parameters that minimized the χ^2_ν of our fit. However, we discovered the SciPy Python module from which we imported *scipy.optimize.curve_fit* [2]. This function allowed us to find the optimal parameter set that minimized our χ^2_ν over a range of parameter values for each parameter in our set. This function also returns a covariance matrix from which we are able to calculate one standard deviation errors on each of our parameters. This standard deviation error calculation is equivalent to starting at our optimal parameters point in our parameter grid and finding the minimum distance we have to travel down the relevant parameter axis to double our minimum χ^2_ν value, which is the classic method of calculating optimal fit parameter error.

Once we have calculated our minimum χ^2_ν, we can begin to interpret the quality of our fit. Namely, if our $\chi^2_\nu \ll 1$, then we have either overestimated our errors or over-fitted and if our $\chi^2_\nu \gg 1$, then we have either underestimated our errors or discovered a discrepancy between our data and what is expected by theory reflecting the inaccuracy of our model.

2. *Residuals*

Another method of fit analysis is a residuals calculation. Here, we subtract our optimal fit curve from our data normalized by the error bars in our data.

The residual for data point y_i is:

$$\epsilon_i(x_i) = \frac{y_i - f(x_i, \alpha^*)}{\sigma_i} \tag{VII.4}$$

where $f(x_i, \alpha^*)$ is the theoretical value at x_i using the best fit parameter set α^*, as determined by our χ^2_ν minimization and σ_i is the error bar of data point y_i.

The residuals add in quadrature to yield our minimum χ^2 value, and while minimizing this sum is important, it is also important that our residuals reflect roughly randomly distributed data around our theoretical predictions. Ideally, the resulting curve should resemble normally distributed noise with mean zero and standard deviation 1. A reasonable residuals curve and minimum χ^2_ν value are strong indications of data that is consistent with theory.

[1] Bhattacharjee, S. M. and Khare, A. (2008), "Fifty Years of the Exact solution of the Two-dimensional Ising Model by Onsager," *Institute of Physics, Sachivalaya Marg.*

[2] community, T. S. (2019), "scipy.optimize.curve_fit," .

[3] Ising, T., Folk, R., kenna, R., Berche, B., and Holovatch, Y. (2017), "The Fate of Ernst Ising and the Fate of his Model," .

[4] Malsagov, M., Karandashev, I., and Kryzhanovsky, B. (2017), "The Analytical Expressions for a Finite-Size 2D Ising Model," .

[5] Stewart, D. (2019), "Phys 382 Ising Model Lab," .